ENGINEERING
ANALYSIS *with*
B O U N D A R Y
E L E M E N T S

Dual boundary element analysis of oblique incident wave passing a thin submerged breakwater

K.H. Chen, J.T. Chen*, C.R. Chou, C.Y. Yueh

Department of Harbor and River Engineering, National Taiwan Ocean University, 20224 Keelung, Taiwan, ROC

Received 30 August 2001; revised 5 March 2002; accepted 29 April 2002

Abstract

In this paper, the dual integral formulation for the modified Helmholtz equation in solving the propagation of oblique incident wave passing a thin barrier (a degenerate boundary) is derived. All the improper integrals for the kernel functions in the dual integral equations are reformulated into regular integrals by integrating by parts and are calculated by means of the Gaussian quadrature rule. The jump properties for the single layer potential, double layer potential and their directional derivatives are examined and the potential distributions are shown. To demonstrate the validity of the present formulation, the transmission and reflection coefficients of oblique incident wave passing a thin rigid barrier are determined by the developed dual boundary element method program. Also, the results are obtained for the cases of wave scattering by a rigid barrier with a finite or zero thickness in a constant water depth and compared with those of experiment and analytical solution using eigenfunction expansion method. Good agreement is observed. © 2002 Elsevier Science Ltd. All rights reserved.

Keywords: Dual boundary element analysis; Obliquewave; Eigenfunction; Modifed Helmholt equation; Thin breakwater

1. Introduction

The boundary element method (BEM), sometimes referred to as the boundary integral equation method, is now establishing a position as an actual alternative to the finite element method in many fields of engineering. The dual boundary element method (DBEM), or the so-called dual boundary integral equation method (DBIEM) developed by Hong and Chen [23], is particularly suitable for the problems with a degenerate boundary. Mathematically speaking, the hypersingular integral equation was first formulated by Hadamard [22] to treat the cylindrical wave equation by the spherical means of descent. In the meantime, Mangler derived the same mathematical form in solving a thin airfoil problem [35]. The improper integral was then defined by Tuck [47] as the 'Hadamard principal value (HPV)'. In aerodynamics, it was termed the 'Mangler's principal value' [35]. Such a nonintegrable kernel naturally arises in the dual integral formulation especially for the problems with a degenerate boundary, e.g. crack problems in elasticity [22,23,43], Darcy flow around a cutoff wall [20], the aerodynamic problem of a thin airfoil

[48], electromagnetic wave impinging on an antenna [41] and acoustic wave impinging on a screen [8,11,12,18,46, 49]. The thin water barrier considered in the present paper is also one case of degenerate boundary. The dual formulation also plays important roles in some other problems, e.g. corner problems [14], adaptive BEM [3,28], degenerate scale problems [4,5], spurious eigenvalues of an interior problem [9,10,50], and fictitious frequencies of an exterior problem [6]. A general application of the hypersingular integral equation in mechanics was discussed in Ref. [37], and a review article on the DBEM was presented in Ref. [7]. Combining the conventional integral equation, e.g. the Green's Identity or Somigliana Identity, with the hypersingular integral equation, we call the two equations 'dual integral equations' according to the symmetry and transpose symmetry properties of the kernels [21,23]. From the above point of view, the definition of the dual integral equations is quite different from the conventional one used in crack elastodynamics by Buecker [2]. The dual equations in the present paper are independent with respect to each other for the undetermined coefficients in the discrete system. The dual integral equations defined by Buecker resulted from the same equation but by collocating different points. The present formulation has a total of four kernel functions, which makes possible a unified theory encompassing different schemes, various derivations and interpretations.

* Corresponding author. Tel.: +886-2-2462-2192x6177; Fax: +886-2-24632375.

E-mail address: jtchen@mail.ntou.edu.tw (J.T. Chen).

For crack problems, a detailed derivation can be found in Ref. [23]. The order of singularity for the kernel in the normal derivative of the double layer potential is stronger than that of the Cauchy type kernel by one. The paradox of the nonintegrable kernel is introduced due to the illegal change of the integral and trace operators from the viewpoint of the dual integral formulation. In order to ensure a finite value, Leibnitz's rule should be considered in the derivative of Cauchy principal value (CPV) so that the boundary term of positive infinity can be included to compensate for the minus infinity. In the last two decades, many researchers have paid attention to regularization techniques [45] for hypersingular and nearly hypersingular integrals. Therefore, the value for the finite part can be determined by means of regularization techniques. Based on the theory of dual integral equations, the DBEM has been implemented [15,16]. The dual integral representation for the Laplace equation was proposed in Ref. [15] and a general purpose program, BEPO2D, was developed. Also, the program for crack problems has been developed by Hong and Chen [23]. Portela extended to solve the crack growth problems [43]. For the Helmholtz equation, the dual formulation was developed by Chen and Chen [12]. In the same way, the acoustic problem of the Helmholtz equation with a screen was also solved successfully using the DBEM program [12]. To the authors' best knowledge, the DBEM for the modified Helmholtz equation of a thin breakwater subject to oblique water wave was not constructed.

Prediction of wave interactions has been studied previously by a number of authors for many kinds of configuration of a water barrier on the basis of linear wave diffraction theory [17,29,38]. Many analytical and numerical solutions have been developed on the basis of the eigenfunction expansion method [24,32–34,44] and the BEM [25,30, 31,39,42,51], respectively. Following the theory of dual integral equations and BEPO2D program developed by Chen and Hong [15,16], the DBEM program has been modified to solve the water wave problem of normal incident water wave past a submerged thin barrier by Yueh and Tsaur [51]. The reflection and transmission of oblique incident water wave past a submerged barrier with a finite width were studied using the conventional BEM under the linear wave theory [30]. In these references, the incident angle of wave, shape of barrier, barrier height, width and slope under various wave conditions have been considered. Nowadays, submerged breakwaters are often constructed to protect a harbor from waves of the open sea. The primary function is to reduce the wave energy transmitted through it and to have the advantages of allowing water circulation, fish passage, providing economical protection. A suitable arrangement of a thin barrier may act as a good model for a breakwater. The effect of such an arrangement on incident wave can be studied by using the DBEM, assuming linear theory for the thin breakwater.

In this paper, we will construct the dual integral formulation for solving the problems of oblique incident wave passing a 'thin' water barrier, which is similar to the acoustic problem with a screen [12] and torsion problem with a cracked bar [13]. Physically speaking, there is no zero thickness breakwater in the real world. But a finite thickness can be modeled as a zero thickness mathematically after comparing the wavelength and the thickness of breakwater. In the literature, a thin breakwater and cutoff wall have been modeled by a zero thickness, by Farina et al. [19] and Lafe et al. [27]. Therefore, thin water barrier and screen can be seen as degenerate boundaries. The governing equation considered here is the modified Helmholtz equation for oblique incident wave passing a thin water barrier instead of the Helmholtz equation for acoustic wave impinging on a screen. The rigid boundary condition of a thin barrier will be considered. All the improper integrals for the kernel functions (*UT* in the singular equation, *LM* in the hypersingular equation) encountered in the dual integral equations using constant element will be reformulated into regular integrals by integrating by parts and will be calculated by the Gaussian quadrature rule. The constant element used in the present paper is a zeroth order boundary element. In aerodynamics, zeroth order boundary element so-called panel method is very popular, e.g. USAERO and PANAIR programs. Since the C^1 continuity of density function in the hypersingular equation is required [26,36], use of the linear element results in an unbounded potential. Also, the corner needs special treatment. These two reasons lead us to use the constant element. The roles of hypersingular integral equation in the DBEM for the problems with a degenerate boundary (thin barrier) will be examined. For the kernels in the dual formulation, we will extend our experiences of the dual formulation on the Laplace equation [16], Helmholtz equation [12] and Navier equation [23] to the modified Helmholtz equation and will examine the potential properties of the four kernel functions. After discretizing the dual integral equations, a DBEM program will be developed to solve the propagation of oblique incident wave passing a thin barrier with a finite or zero thickness. The results will be compared with those of experiment and analytical solution by using the eigenfunction expansion method.

2. Dual integral formulation for the scattering wave problem with a thin water barrier (a degenerate boundary)

Consider a vertical thin barrier parallel to the *z*-axis as shown in Fig. 1. A wave train with a frequency σ propagates towards the barrier with an angle θ in a constant water depth *h*. Assuming inviscid, incompressible fluid and irrotational flow, the wave field may be represented by the velocity potential $\Phi(x, y, z, t)$ which satisfies the Laplace equation as

$$\nabla^2 \Phi(x, y, z, t) = 0. \qquad (1)$$

According to the uniformity of the water depth in the *z*-axis

(S denotes the normal boundary, C^+ and C^- denote the degenerate boundary)
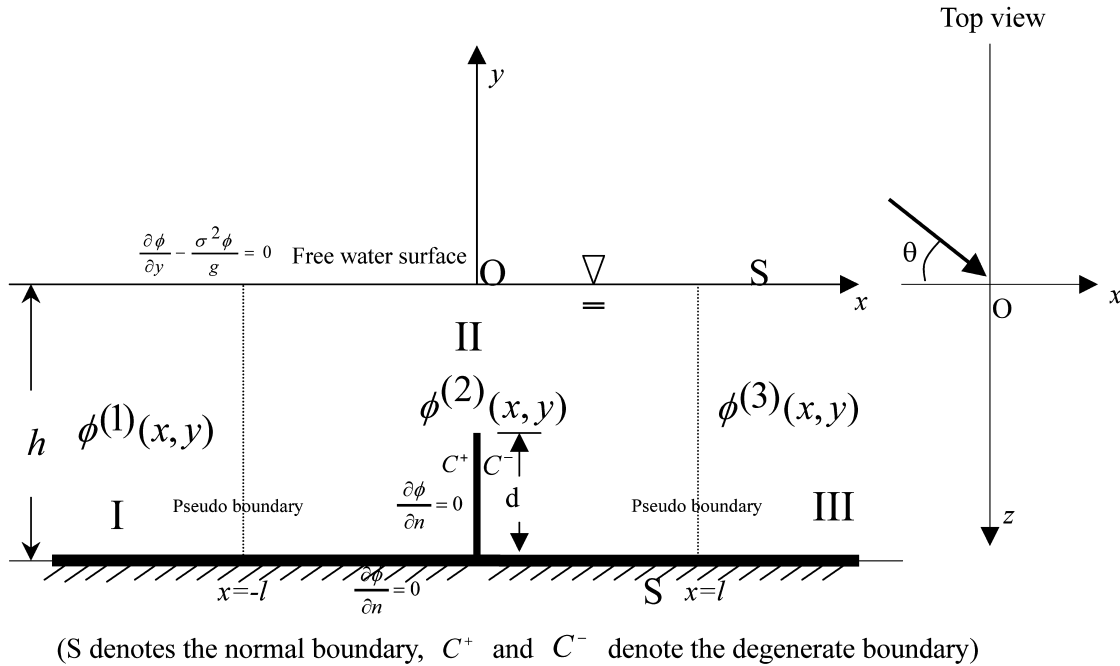
Fig. 1. Definition sketch of the water scattering problem of oblique incident wave past a rigid thin-barrier.

and the periodicity in time, the potential $\Phi(x, y, z, t)$ of fluid motion can be expressed as:

$$\Phi(x, y, z, t) = \phi(x, y)e^{i(\lambda z - \sigma t)} \tag{2}$$

where $\lambda = k \sin(\theta)$ and k is the wave number which satisfies the dispersion relation:

$$\sigma^2 = gk \tanh(kh), \tag{3}$$

in which g is the acceleration of gravity. The unknown function, $\phi(x, y)$, describes the fluctuation of the potential on the xy plane. Substitution of Eqs. (2) into (1) yields the modified Helmholtz equation as follows:

$$\nabla^2 \phi(x, y) - \lambda^2 \phi(x, y) = 0, \quad (x, y) \text{ in } D, \tag{4}$$

where D is the domain of interest. The boundary conditions of the interested domain are summarized as:

1. The linearized free water surface boundary condition:

$$\frac{\partial \phi}{\partial y} - \frac{\sigma^2 \phi}{g} = 0. \tag{5}$$

2. Seabed and breakwater boundary conditions:

$$\frac{\partial \phi}{\partial n} = 0, \tag{6}$$

   where n is boundary normal vector.
3. Radiation condition at infinity:

$$\lim_{x \to \infty} x^{1/2} \left(\frac{\partial \phi}{\partial x} - ik\phi \right) = 0. \tag{7}$$

4. The boundary conditions on the fictitious interfaces:
   For the infinite strip problem, the domain can be divided

into three regions after introducing two pseudo-boundaries on both sides of the barrier, $x = \pm l$, as shown in Fig. 1. The potential in the region I without energy loss can be expressed as:

$$\phi^{(1)}(x, y) = (e^{i\eta(x+l)} + R\, e^{-i\eta(x+l)}) \frac{\cosh(k(h - y))}{\cosh(kh)} \tag{8}$$

where the superscript of ϕ denotes the region number, R is the reflection coefficient and $\eta = k \cos(\theta)$. The potential in the region III without energy loss can be expressed as:

$$\phi^{(3)}(x, y) = T\, e^{i\eta(x-l)} \frac{\cosh(k(h - y))}{\cosh(kh)}, \tag{9}$$

where T is the transmission coefficient.

The boundary conditions on the fictitious interfaces are

$$\phi^{(1)}(-l, y) = \phi^{(2)}(-l, y) \tag{10}$$

$$\left. \frac{\partial \phi^{(1)}}{\partial x} \right|_{x=-l} = \left. \frac{\partial \phi^{(2)}}{\partial x} \right|_{x=-l} \tag{11}$$

$$\phi^{(3)}(l, y) = \phi^{(2)}(l, y) \tag{12}$$

$$\left. \frac{\partial \phi^{(3)}}{\partial x} \right|_{x=l} = \left. \frac{\partial \phi^{(2)}}{\partial x} \right|_{x=l}. \tag{13}$$

According to Eqs. (8)–(10) and (12), we can derive the reflection and transmission coefficients as follows:

$$R = -1 + \frac{k}{n_0 \sinh(kh)} \int_{-h}^{0} \phi^{(2)}(-l, y)\cosh(k(h - y))\mathrm{d}y \tag{14}$$

$$T = \frac{k}{n_0 \sinh(kh)} \int_{-h}^{0} \phi^{(2)}(l, y)\cosh(k(h - y))\mathrm{d}y \tag{15}$$

where

$$n_0 = \frac{1}{2}\left(1 + \frac{2kh}{\sinh(2kh)}\right).$$

The first equation of the dual boundary integral equations for the domain point can be derived from the Green's third identity [30]:

$$2\pi\phi(\tilde{x}) = \int_{B} T(\tilde{s}, \tilde{x})\phi(\tilde{s})\mathrm{d}B(\tilde{s}) - \int_{B} U(\tilde{s}, \tilde{x})\frac{\partial\phi(\tilde{s})}{\partial n_{\tilde{s}}}\mathrm{d}B(\tilde{s}),$$
$$\tilde{x} \in D, \tag{16}$$

where $\tilde{x}$ is the field point ($\tilde{x} = (x, y)$), $\tilde{s}$ is the source point, and $T(\tilde{s}, \tilde{x})$ is defined by

$$T(\tilde{s}, \tilde{x}) \equiv \frac{\partial U(\tilde{s}, \tilde{x})}{\partial n_{\tilde{s}}}, \tag{17}$$

in which $n_{\tilde{s}}$ denotes the normal vector at the boundary point $\tilde{s}$, and $U(\tilde{s}, \tilde{x})$ is the fundamental solution which satisfies

$$\nabla^2 U(\tilde{x}, \tilde{s}) - \lambda^2 U(\tilde{x}, \tilde{s}) = \delta(\tilde{x} - \tilde{s}), \quad \tilde{x} \in D. \tag{18}$$

In Eq. (18), $\delta(\tilde{x} - \tilde{s})$ is the Dirac-delta function. After taking normal derivative with respect to Eq. (16) for a thin barrier problem, the second equation of the dual boundary integral equations for the domain point is derived:

$$2\pi\frac{\partial\phi(\tilde{x})}{\partial n_{\tilde{x}}} = \int_{B} M(\tilde{s}, \tilde{x})\phi(\tilde{s})\mathrm{d}B(\tilde{s}) - \int_{B} L(\tilde{s}, \tilde{x})\frac{\partial\phi(\tilde{s})}{\partial n_{\tilde{s}}}\mathrm{d}B(\tilde{s}),$$
$$\tilde{x} \in D, \tag{19}$$

where

$$L(\tilde{s}, \tilde{x}) \equiv \frac{\partial U(\tilde{s}, \tilde{x})}{\partial n_{\tilde{x}}}, \tag{20}$$

$$M(\tilde{s}, \tilde{x}) \equiv \frac{\partial^2 U(\tilde{s}, \tilde{x})}{\partial n_{\tilde{x}}\,\partial n_{\tilde{s}}}, \tag{21}$$

in which $n_{\tilde{x}}$ represents the normal vector of $\tilde{x}$. The explicit forms for the four kernel functions are shown in Table 1. By moving the field point $\tilde{x}$ in Eqs. (16) and (19) to the boundary, the dual boundary integral equations for the boundary point can be obtained as follows:

$$\pi\phi(\tilde{x}) = \mathrm{CPV}\int_{B} T(\tilde{s}, \tilde{x})\phi(\tilde{s})\mathrm{d}B(\tilde{s})$$
$$- \mathrm{RPV}\int_{B} U(\tilde{s}, \tilde{x})\frac{\partial\phi(\tilde{s})}{\partial n_{\tilde{s}}}\mathrm{d}B(\tilde{s}), \quad \tilde{x} \in B, \tag{22}$$

$$\pi\frac{\partial\phi(\tilde{x})}{\partial n_{\tilde{x}}} = \mathrm{HPV}\int_{B} M(\tilde{s}, \tilde{x})\phi(\tilde{s})\mathrm{d}B(\tilde{s})$$
$$- \mathrm{CPV}\int_{B} L(\tilde{s}, \tilde{x})\frac{\partial\phi(\tilde{s})}{\partial n_{\tilde{s}}}\mathrm{d}B(\tilde{s}), \quad \tilde{x} \in B, \tag{23}$$

where RPV is the Riemann principal value, CPV is the Cauchy principal value and HPV is the Hadamard (Mangler) principal value.

It must be noted that Eq. (23) can be derived simply by applying a normal derivative operator with respect to Eq. (22). Differentiation of the CPV should be carried out carefully by using Leibnitz's rule. The commutative property provides us with two alternatives for calculating the HPV in a similar way used for crack problems [23]. For the problem including a normal boundary S and degenerate boundaries C^+ and C^- on the both sides of a thin barrier, i.e. $B = S + C^+ + C^-$, Eqs. (22) and (23) can be reformulated as follows.

For $\tilde{x} \in S$, Eqs. (22) and (23) become

$$\pi\phi(\tilde{x}) = \mathrm{CPV}\int_{S} T(\tilde{s}, \tilde{x})\phi(\tilde{s})\mathrm{d}B(\tilde{s})$$
$$- \mathrm{RPV}\int_{S} U(\tilde{s}, \tilde{x})\frac{\partial\phi(\tilde{s})}{\partial n_{\tilde{s}}}\mathrm{d}B(\tilde{s})$$
$$+ \int_{C^+} T(\tilde{s}, \tilde{x})\Delta\phi(\tilde{s})\mathrm{d}B(\tilde{s})$$
$$- \int_{C^+} U(\tilde{s}, \tilde{x})\sum\frac{\partial\phi(\tilde{s})}{\partial n_{\tilde{s}}}\mathrm{d}B(\tilde{s}) \tag{24}$$

$$\pi\frac{\partial\phi(\tilde{x})}{\partial n_{\tilde{x}}} = \mathrm{HPV}\int_{S} M(\tilde{s}, \tilde{x})\phi(\tilde{s})\mathrm{d}B(\tilde{s})$$
$$- \mathrm{CPV}\int_{S} L(\tilde{s}, \tilde{x})\frac{\partial\phi(\tilde{s})}{\partial n_{\tilde{s}}}\mathrm{d}B(\tilde{s})$$
$$+ \int_{C^+} M(\tilde{s}, \tilde{x})\Delta\phi(\tilde{s})\mathrm{d}B(\tilde{s})$$
$$- \int_{C^+} L(\tilde{s}, \tilde{x})\sum\frac{\partial\phi(\tilde{s})}{\partial n_{\tilde{s}}}\mathrm{d}B(\tilde{s}), \tag{25}$$

where

$$\Delta\phi(\tilde{s}) \equiv \phi(\tilde{s}^+) - \phi(\tilde{s}^-) \tag{26}$$

$$\sum\frac{\partial\phi}{\partial n}(\tilde{s}) \equiv \frac{\partial\phi}{\partial n}(\tilde{s}^+) + \frac{\partial\phi}{\partial n}(\tilde{s}^-). \tag{27}$$

For $\tilde{x} \in C^+$, Eqs. (22) and (23) reduce to

$$\pi\sum\phi(\tilde{x}) = \mathrm{CPV}\int_{C^+} T(\tilde{s}, \tilde{x})\Delta\phi(\tilde{s})\mathrm{d}B(\tilde{s})$$
$$- \mathrm{RPV}\int_{C^+} U(\tilde{s}, \tilde{x})\sum\frac{\partial\phi(\tilde{s})}{\partial n_{\tilde{s}}}\mathrm{d}B(\tilde{s})$$
$$+ \int_{S} T(\tilde{s}, \tilde{x})\phi(\tilde{s})\mathrm{d}B(\tilde{s}) - \int_{S} U(\tilde{s}, \tilde{x})\frac{\partial\phi(\tilde{s})}{\partial n_{\tilde{s}}}\mathrm{d}B(\tilde{s}), \tag{28}$$

Table 1
The properties of the kernel functions for the modified Helmholtz equation

Kernel function $K(\tilde{s},\tilde{x})$	$U(\tilde{s},\tilde{x})$	$T(\tilde{s},\tilde{x})$	$L(\tilde{s},\tilde{x})$	$M(\tilde{s},\tilde{x})$
Explicit forms	$U(\mathbf{s},\mathbf{x}) = iD_0^{(1)}(\lambda r)$	$T(\mathbf{s},\mathbf{x}) = -i\lambda D_1^{(2)}(\lambda r)\frac{y_i n_i}{r}$	$L(\mathbf{s},\mathbf{x}) = i\lambda D_1^{(2)}(\lambda r)\frac{y_i\bar{n}_i}{r}$	$M(\mathbf{s},\mathbf{x}) = -i\lambda\left\{\lambda\frac{D_2^{(1)}(\lambda r)}{r^2}y_iy_jn_i\bar{n}_j + \frac{D_1^{(2)}(\lambda r)}{r}n_i\bar{n}_i\right\}$
Order of singularity	O(ln r) weak	O(1/r) strong	O(1/r) strong	$O(1/r^2)$ hypersingular
Symmetry	$U(\tilde{x},\tilde{s})$	$T(\tilde{x},\tilde{s})$	$L(\tilde{x},\tilde{s})$	$M(\tilde{x},\tilde{s})$
Density function $v(\tilde{s})$	$\partial\phi/\partial n$	ϕ	$\partial\phi/\partial n$	ϕ
Potential type	Single layer	Double layer	Normal derivative of single layer	Normal derivative of double layer
$\int K(\tilde{s},\tilde{x})v(\tilde{s})dB(\tilde{s})$ continuity across boundary	Continuous	Discontinuous	Discontinuous	Psuedo-continuous
Jump value	No jump	$2\pi\phi$	$2\pi(\partial\phi/\partial n)$	No jump
Principal value	Riemann	Cauchy	Cauchy	Hadamard

$D_n^{(1)}(\lambda r)$ is the first kind of nth order modified Hankel function, $\bar{n}_i$ and $\bar{t}_i$ denote the ith component of normal and tangent vectors on $\tilde{x}$, respectively.

$$\pi\Delta\frac{\partial\phi(\tilde{x})}{\partial n_{\tilde{x}}} = \text{HPV}\int_{C^+} M(\tilde{s},\tilde{x})\Delta\phi(\tilde{s})dB(\tilde{s})$$

$$- \text{CPV}\int_{C^+} L(\tilde{s},\tilde{x})\sum\frac{\partial\phi(\tilde{s})}{\partial n_{\tilde{s}}}dB(\tilde{s})$$

$$+ \int_S M(\tilde{s},\tilde{x})\phi(\tilde{s})dB(\tilde{s}) - \int_S L(\tilde{s},\tilde{x})\frac{\partial\phi(\tilde{s})}{\partial n_{\tilde{s}}}dB(\tilde{s}),$$

$$(29)$$

where

$$\sum\phi(\tilde{s}) \equiv \phi(\tilde{s}^+) + \phi(\tilde{s}^-) \tag{30}$$

$$\Delta\frac{\partial\phi}{\partial n}(\tilde{s}) \equiv \frac{\partial\phi}{\partial n}(\tilde{s}^+) - \frac{\partial\phi}{\partial n}(\tilde{s}^-). \tag{31}$$

Eqs. (26), (27), (30) and (31) indicate that the unknowns on the degenerate boundary double, and that the additional hypersingular integral equation, Eq. (19), is correspondingly necessary, i.e. the dual boundary integral equations can provide us with sufficient constraint relations for the doubled boundary unknowns on the degenerate boundary.

3. On the four kernel functions and their potentials

The four kernel functions, $U(\tilde{s},\tilde{x})$, $T(\tilde{s},\tilde{x})$, $L(\tilde{s},\tilde{x})$ and $M(\tilde{s},\tilde{x})$, in the dual integral equation shave different orders of singularity when $\tilde{x}$ approaches $\tilde{s}$. The order of singularity and the symmetry properties for the four kernel functions and the continuous properties of the potentials across the boundary resulting from the four kernel functions are summarized in Table 1. In Table 1, not only the normal derivatives for the single and double layer potentials, but also the tangential derivatives are considered. For the regular elements, no special treatment is needed since the Gaussian quadrature rule can be directly employed. Without loss of generality, the four improper integrals for the singular elements obtained by using constant element scheme after coordinate transformation can be formulated into the following regular integrals:

(1) $U(\tilde{s},\tilde{x})$ kernel:

$$\text{diag}([U]) = i\lim_{\epsilon\to 0}\int_{-0.5l}^{0.5l} D_0^{(1)}(\lambda\sqrt{s^2+\epsilon^2})ds$$

$$= i\lim_{\epsilon\to 0}\left\{\int_{-0.5l}^{-\sqrt{\epsilon}} D_0^{(1)}(\lambda|s|)ds\right.$$

$$+ \int_{-\sqrt{\epsilon}}^{\sqrt{\epsilon}} (-i)\ln(\lambda\sqrt{s^2+\epsilon^2})ds + \left.\int_{\sqrt{\epsilon}}^{0.5l} D_0^{(1)}(\lambda s)ds\right\}$$

$$= i\lim_{\epsilon\to 0}\left\{\int_{-0.5l}^{-\sqrt{\epsilon}} D_0^{(1)}(\lambda|s|)ds + 0 + \int_{\sqrt{\epsilon}}^{0.5l} D_0^{(1)}(\lambda s)ds\right\}$$

$$= i\left\{D_0^{(1)}\left(\frac{\lambda l}{2}\right)l - \lambda\int_{-0.5l}^{0.5l} D_1^{(2)}(\lambda|s|)|s|ds\right\}, \tag{32}$$

where $i^2 = -1$, diag([U]) denotes the diagonal element of the influence matrix $[U]$ (which will be elaborated on later in Eq. (36)), $D_0^{(1)}(\lambda s)$ is the first kind of the zeroth order modified Hankel function, l is the element length and the coordinate of the collocation point $\tilde{x}$ is (0,0).

(2) $T(\tilde{s}, \tilde{x})$ kernel:

$$\text{diag}([T]) = i\lambda \lim_{\epsilon \to 0} \int_{-0.5l}^{0.5l} D_1^{(2)}(\lambda\sqrt{s^2 + \epsilon^2}) \frac{\epsilon}{\sqrt{s^2 + \epsilon^2}} ds$$

$$= i\lambda \lim_{\epsilon \to 0} \int_{-\sqrt{\epsilon}}^{\sqrt{\epsilon}} \frac{-i(1)}{\lambda\sqrt{s^2 + \epsilon^2}} \frac{\epsilon}{\sqrt{s^2 + \epsilon^2}} ds$$

$$= \lim_{\epsilon \to 0} \arctan \frac{s}{\epsilon}\Big|_{-\sqrt{\epsilon}}^{\sqrt{\epsilon}} = \pi, \quad (33)$$

where $D_1^{(2)}(\lambda s)$ is the second kind of the first order modified Hankel function and $[T]$ is the influence matrix (which will be elaborated on later in Eq. (37)).

(3) $L(\tilde{s}, \tilde{x})$ kernel:

$$\text{diag}([L]) = i\lambda \lim_{\epsilon \to 0} \int_{-0.5l}^{0.5l} D_1^{(2)}(\lambda\sqrt{s^2 + \epsilon^2}) \frac{-\epsilon}{\sqrt{s^2 + \epsilon^2}} ds$$

$$= \lim_{\epsilon \to 0} - i\lambda \int_{-\sqrt{\epsilon}}^{\sqrt{\epsilon}} \frac{-i(1)}{\lambda\sqrt{s^2 + \epsilon^2}} \frac{\epsilon}{\sqrt{s^2 + \epsilon^2}} ds$$

$$= -\pi \quad (34)$$

where $[L]$ is the influence matrix (which will be elaborated on later in Eq. (38)).

(4) $M(\tilde{s}, \tilde{x})$ kernel:

$$\text{diag}(M) = -i\lambda \lim_{\epsilon \to 0} \int_{-0.5l}^{0.5l} \lambda \frac{D_2^{(1)}(\lambda\sqrt{s^2 + \epsilon^2})}{s^2 + \epsilon^2}(-\epsilon)$$

$$\times(-\epsilon) + \frac{D_2^{(1)}(\lambda\sqrt{s^2 + \epsilon^2})}{\sqrt{s^2 + \epsilon^2}} ds$$

$$= -i\lambda\left\{ - 2D_1^{(2)}\left(\frac{\lambda l}{2}\right) + \lambda\left[D_0^{(1)}\left(\frac{\lambda l}{2}\right) l \right. \right.$$

$$\left. \left. - \lambda \int_{-0.5l}^{0.5l} D_1^{(2)}(\lambda|s|)|s| ds \right] \right\}, \quad (35)$$

where $D_2^{(1)}(\lambda s)$ is the first kind of the second order modified Hankel function and $[M]$ is the influence matrix (which will be elaborated on later in Eq. (39)). After the above manipulations, the improper integrals, including weak ($U(\tilde{s}, \tilde{x})$), strong ($T(\tilde{s}, \tilde{x}), L(\tilde{s}, \tilde{x})$) and superstrong ($M(\tilde{s}, \tilde{x})$) singularities, reduce to regular integrals and are calculated using the Gaussian quadrature rule.

The potentials of the six kernel functions, $U(\tilde{s}, \tilde{x}), T(\tilde{s}, \tilde{x}),$ $L(\tilde{s}, \tilde{x}), M(\tilde{s}, \tilde{x}), L^t(\tilde{s}, \tilde{x})$ and $M^t(\tilde{s}, \tilde{x})$ in Table 1, induced by the constant singularity source distributed along the boundary from $\tilde{s} = (-0.5, 0)$ to $\tilde{s} = (0.5, 0)$ are shown in

Fig. 2 for value of $\lambda = 0.01$. The behavior of the single layer potential ($U(\tilde{s}, \tilde{x})$ kernel), the double layer potential ($T(\tilde{s}, \tilde{x})$ kernel), the normal derivative of the single layer potential ($L^n(\tilde{s}, \tilde{x})$ kernel), the normal derivative of the double layer potential ($M^n(\tilde{s}, \tilde{x})$ kernel), the tangential derivative of the single layer potential ($L^t(\tilde{s}, \tilde{x})$ kernel) and the tangential derivative of the double layer potential ($M^t(\tilde{s}, \tilde{x})$ kernel) are all shown in the figures where only real part is considered. It is found that the asymptotic behavior of the real part of the kernels for the modified Helmholtz equation in Fig. 2 is similar to that of the Laplace equation in Refs. [15,16] as expected. The continuous behaviors of the single layer potential ($U(\tilde{s}, \tilde{x})$ kernel) and the normal derivative of the double layer potential ($M(\tilde{s}, \tilde{x})$ kernel) are displayed in this figure. The jump behaviors across the boundary connected from $\tilde{s} = (-0.5, 0)$ to $\tilde{s} = (0.5, 0)$ can be observed for the double layer potential ($T(\tilde{s}, \tilde{x})$ kernel) and the normal derivative of the single layer potential ($L(\tilde{s}, \tilde{x})$ kernel). Also, the dipole and quadrapole source structures are found. By employing the singular solutions, the strength of the
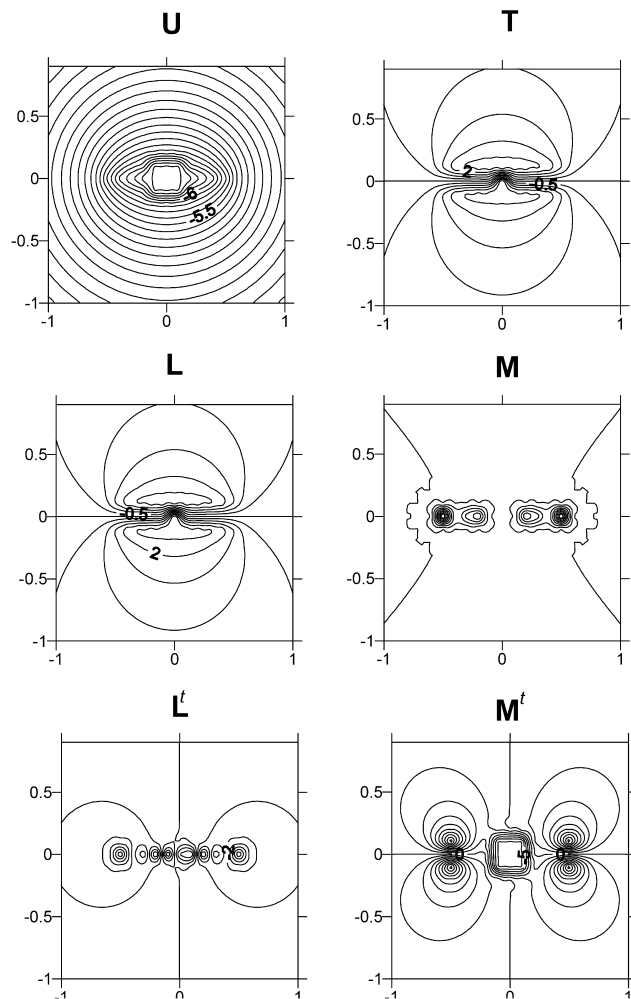
Fig. 2. Contours of the real-part potentials resulting from the six kernel functions for $\lambda = 0.01$.

(a)   UT Method (normal boundary)+LM
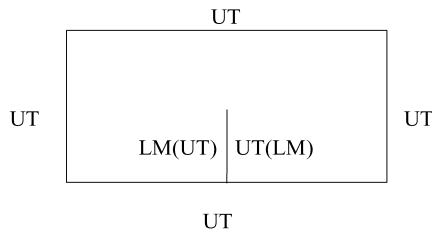
(b)   LM Method (normal boundary)+UT
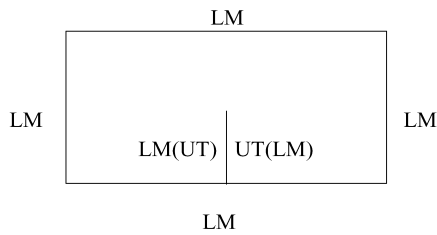
Fig. 3. Two alternative approaches.

$h=10$ m, $d=7.5$ m, $b=10$ and 5 m, $l=20$ m

Fig. 4. The boundary element mesh for the first example.

singularity can be determined by satisfying the boundary conditions.

4. Dual boundary element method for a thin barrier

By discretizing Eqs. (22) and (23) using boundary elements, we can obtain the transcendental equation as follows:

$$[\bar{T}_{ij}(\lambda)]\{\phi_j\} = [U_{ij}(\lambda)]\left\{\left(\frac{\partial \phi}{\partial n}\right)_j\right\},$$

$$[M_{ij}(\lambda)]\{\phi_j\} = [\bar{L}_{ij}(\lambda)]\left\{\left(\frac{\partial \phi}{\partial n}\right)_j\right\},$$

where the elements of the four influence matrices are

$$U_{ij}(\lambda) = \text{RPV}\int_{B_j} U(\tilde{s}_j, \tilde{x}_i)\mathrm{d}B(\tilde{s}_j), \tag{36}$$

$$\bar{T}_{ij}(\lambda) = -\pi\delta_{ij} + \text{CPV}\int_{B_j} T(\tilde{s}_j, \tilde{x}_i)\mathrm{d}B(\tilde{s}_j), \tag{37}$$

$$\bar{L}_{ij}(\lambda) = \pi\delta_{ij} + \text{CPV}\int_{B_j} L(\tilde{s}_j, \tilde{x}_i)\mathrm{d}B(\tilde{s}_j), \tag{38}$$

$$M_{ij}(\lambda) = \text{HPV}\int_{B_j} M(\tilde{s}_j, \tilde{x}_i)\mathrm{d}B(\tilde{s}_j), \tag{39}$$

in which λ is imbedded in the elements of each matrix, $\tilde{x}_i$ is the ith collocation point, $\mathrm{d}B(\tilde{s}_j)$ is the jth integration element and B_j denotes the jth boundary element. After combining the dual equations on the degenerate boundary when $\tilde{x}$ collocates on C^+ or C^-, the singular system of the four
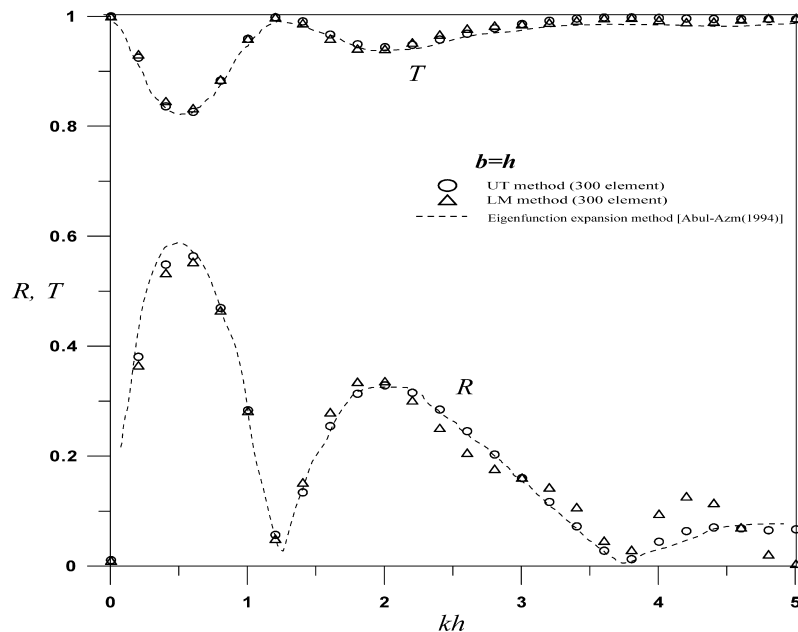
Fig. 5. The reflection and transmission coefficients versus kh for $\theta = 0°$ ($b/h = 1$) (example 1).
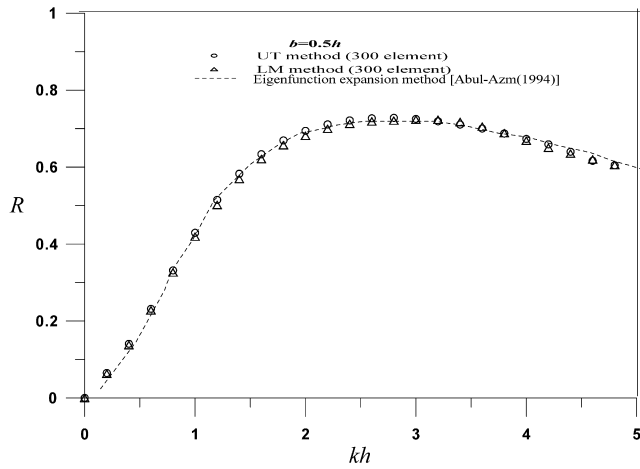
Fig. 6. The reflection and transmission coefficients versus kh for $\theta = 75°$ ($b/h = 0.5$) (example 1).

influence matrices are desingularized. Since either one of the two equations, UT or LM, for the normal boundary S can be selected, two alternative approaches, $UT + LM$ and $LM + UT$ in Fig. 3, are proposed.

The $UT + LM$ method employs the following equation:

$$
\begin{bmatrix}
T_{i_S j_S} & T_{i_S j_{C^+}} & T_{i_S j_{C^-}} \\
T_{i_{C^+} j_S} & T_{i_{C^+} j_{C^+}} & T_{i_{C^+} j_{C^-}} \\
M_{i_{C^+} j_S} & M_{i_{C^+} j_{C^+}} & M_{i_{C^+} j_{C^-}}
\end{bmatrix}
\begin{Bmatrix}
\phi_{j_S} \\
\phi_{j_{C^+}} \\
\phi_{j_{C^-}}
\end{Bmatrix}
$$
$$
=
\begin{bmatrix}
U_{i_S j_S} & U_{i_S j_{C^+}} & U_{i_S j_{C^-}} \\
U_{i_{C^+} j_S} & U_{i_{C^+} j_{C^+}} & U_{i_{C^+} j_{C^-}} \\
L_{i_{C^+} j_S} & L_{i_{C^+} j_{C^+}} & L_{i_{C^+} j_{C^-}}
\end{bmatrix}
\begin{Bmatrix}
\frac{\partial \phi}{\partial n} {}_{j_S} \\
\frac{\partial \phi}{\partial n} {}_{j_{C^+}} \\
\frac{\partial \phi}{\partial n} {}_{j_{C^-}}
\end{Bmatrix},
\tag{40}
$$

where i_S and i_{C^+} denote the collocation points on the S and C^+ boundaries, respectively, and j_S and j_{C^+} denote the element ID on the S and C^+ boundaries, respectively. Also,
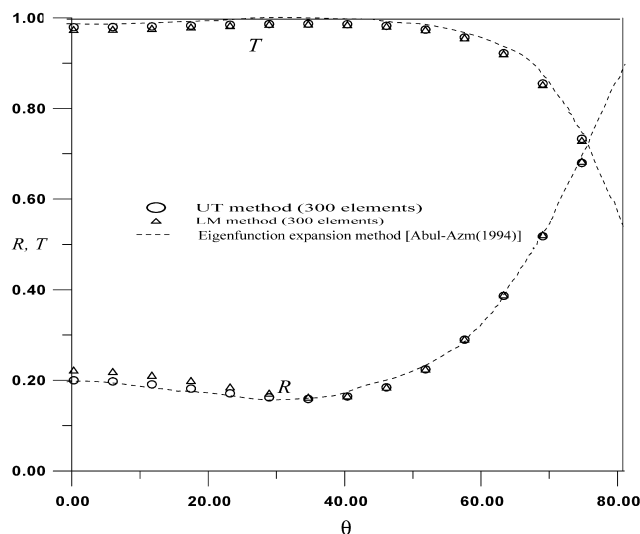
Fig. 7. The reflection and transmission coefficients versus θ for $kh = 1.5$ ($b/h = 1$) (example 1).
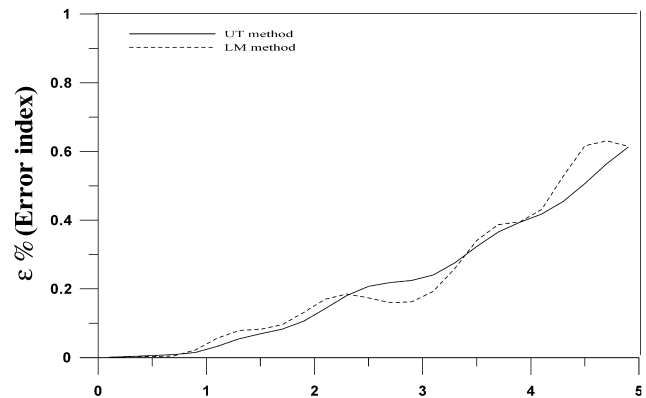
Fig. 8. The error index, $\epsilon\%$, versus kh for $\theta = 0°$ ($b/h = 1$) (example 1).

$LM + UT$ method can solve the degenerate boundary problem by using

$$
\begin{bmatrix}
M_{i_S j_S} & M_{i_S j_{C^+}} & M_{i_S j_{C^-}} \\
T_{i_{C^+} j_S} & T_{i_{C^+} j_{C^+}} & T_{i_{C^+} j_{C^-}} \\
M_{i_{C^+} j_S} & M_{i_{C^+} j_{C^+}} & M_{i_{C^+} j_{C^-}}
\end{bmatrix}
\begin{Bmatrix}
\phi_{j_S} \\
\phi_{j_{C^+}} \\
\phi_{j_{C^-}}
\end{Bmatrix}
$$
$$
=
\begin{bmatrix}
L_{i_S j_S} & L_{i_S j_{C^+}} & L_{i_S j_{C^-}} \\
U_{i_{C^+} j_S} & U_{i_{C^+} j_{C^+}} & U_{i_{C^+} j_{C^-}} \\
L_{i_{C^+} j_S} & L_{i_{C^+} j_{C^+}} & L_{i_{C^+} j_{C^-}}
\end{bmatrix}
\begin{Bmatrix}
\frac{\partial \phi}{\partial n} {}_{j_S} \\
\frac{\partial \phi}{\partial n} {}_{j_{C^+}} \\
\frac{\partial \phi}{\partial n} {}_{j_{C^-}}
\end{Bmatrix}.
\tag{41}
$$

The main difference between Eqs. (40) and (41) is the constraint obtained by collocating the points on the normal boundary (S), using the UT and LM equations, respectively.

5. Illustrative examples

To demonstrate the validity of the dual integral formulation, two examples are given as follows.

5.1. Example 1: a barrier with finite thickness

An example given by Abul-Azm [1] with geometry
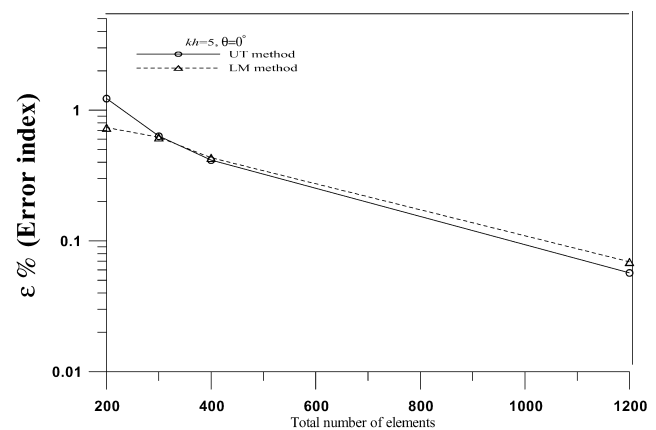
Fig. 9. The error index, $\epsilon\%$, versus the number of elements for the higher wave number ($kh = 5$, $b/h = 1$) (example 1).
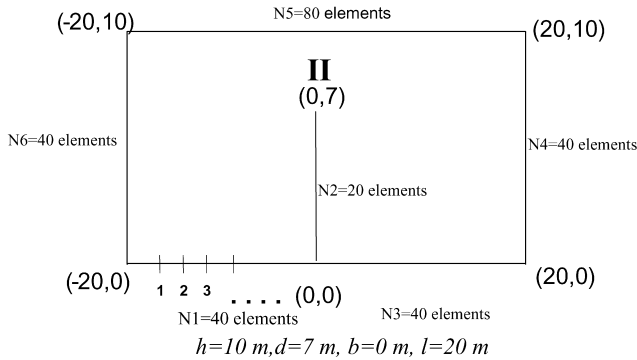
Fig. 10. The boundary element mesh for the second example.

shown in Fig. 4 is considered. According to several numerical experiments, the 20 m length of each pseudo-boundary is adopted which is double of water depth. In this case, the width to length ratio (b/h) is 1 or 0.5, and the submergence ratio (d/h) is 0.75. The boundary mesh of the scattering water wave problem is shown in Fig. 4. By using the formulations (UT method or LM method alone), the reflection and transmission coefficients are plotted against kh for the normal incident wave, $\theta = 0°$ in Fig. 5 ($b/h = 1$) and $\theta = 75°$ in Fig. 6 ($b/h = 0.5$). The reflection and transmission coefficients are plotted versus the angle of incidence (θ) for $kh = 1.5$ as shown in Fig. 7 ($b/h = 1$). The results correlate well with the eigenfunction expansion method by Abul-Azm [1]. The error index, $\epsilon\% = (R^2 + T^2 - 1)100\%$, for conservation of energy between the numerical solution and analytical solution, versus kh for $\theta = 0°$ is plotted in Fig. 8, respectively. To see the sensitivity analysis of results due to numerical parameters particularly for the case of higher wave number, the error index, $\epsilon\%$, is plotted versus number of elements for the

higher wave number ($kh = 5$) as shown in Fig. 9. Two methods, UT and LM formulations, were employed. It is found that the results of these two methods match well except on the region of the higher wave number. The discrepancy of Fig. 5 in the range of higher wave number between the eigenfunction expansion and our results can be attributed to the same number of boundary elements for all the cases of different wave numbers in our method. The case of higher wave number needs more number of elements in the BEM to improve the better result or to employ higher-order element. However, the eigenfunction expansion method does not need boundary elements.

5.2. Example 2: a thin barrier

An example given by Losada et al. [34] is considered. According to several numerical experiments, the 20 m length of each pseudo-boundary is adopted which is double of water depth. The submergence ratio (d/h) is 0.7 and the barrier is modeled as zero thickness, i.e. the boundary of barrier is degenerate. The boundary mesh is shown in Fig. 10. The two methods (UT method or LM method alone) will fail as the thickness becomes zero or near zero. Dual formulation is the key to solve the problem. To understand the ill-conditioned behavior of the algebraic equation due to the near-zero thickness, b, the solutions with different thicknesses are plotted in Fig. 11. Oscillation phenomenon is found. By employing the dual formulation, the reflection and transmission coefficients are plotted against kh for $\theta = 0°$ in Fig. 12. The results were compared with those of the eigenfunction expansion method by Losada et al. [34] and the experimental data by Ogilvie et al. [34,40]. Good agreement among the three solutions was found. The reflection and transmission coefficients are plotted versus
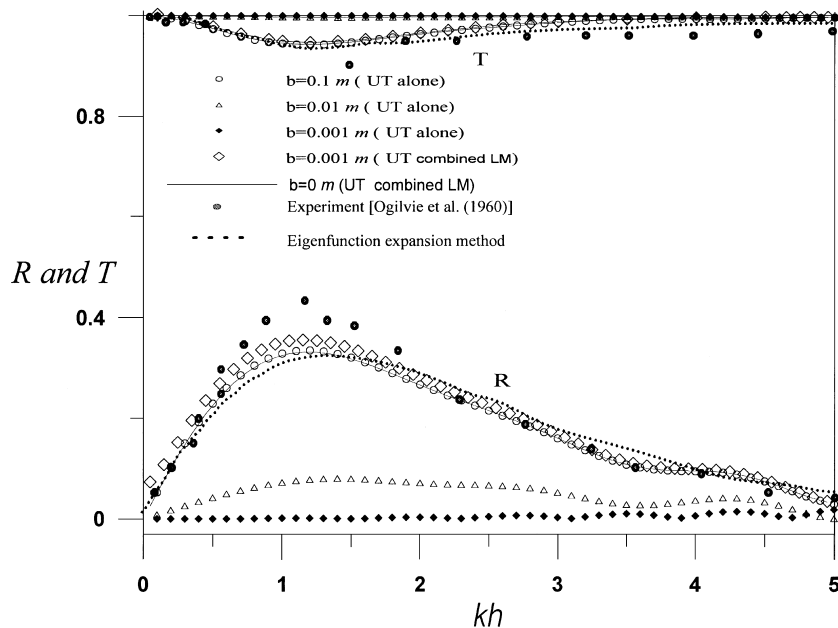
Fig. 11. The reflection and transmission coefficients versus kh with different thicknesses for $\theta = 0°$ (example 2).
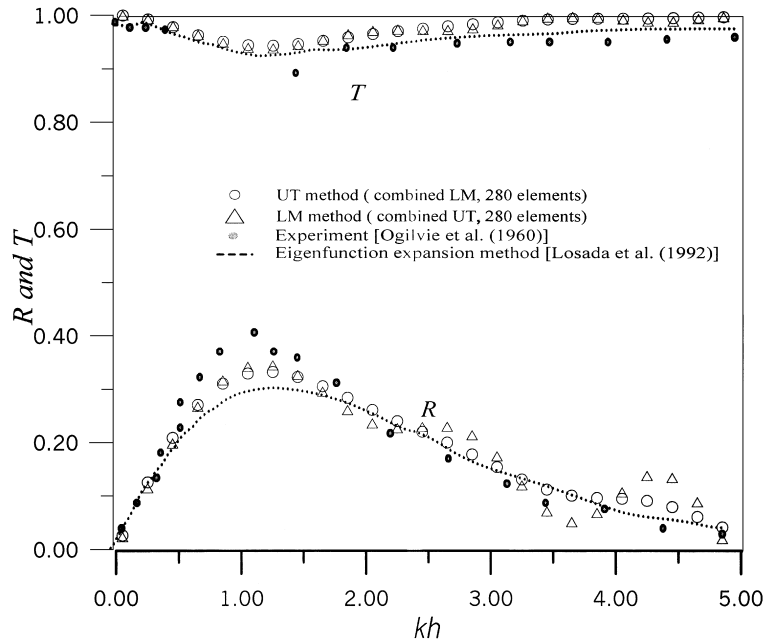
Fig. 12. The reflection and transmission coefficients versus *kh* for $\theta = 0°$ (example 2).
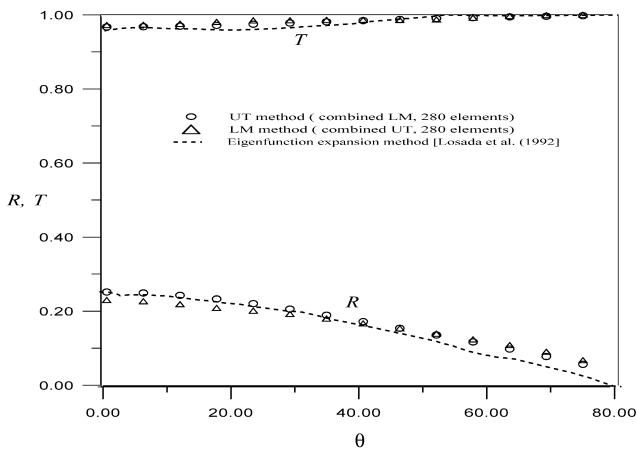
Fig. 13. The reflection and transmission coefficients versus θ for $kh = 2.136$ (example 2).

the angle of incidence (θ) for $kh = 2.136$ as shown in Fig. 13. The two solutions, $UT + LM$ and $LM + UT$ approaches, match well with the eigenfunction solution. The error index, $\epsilon\%$, versus kh for $\theta = 0°$ is plotted in Fig. 14, respectively. To see the sensitivity analysis of results due to numerical parameters particularly for the case of higher wave number, the error index, $\epsilon\%$, is plotted versus the number of elements for the higher wave number ($kh = 5$) as shown in Fig. 15. Two methods, UT and LM formulations, were employed. It is found that the results of two methods match well except on the region of the higher wave number. The discrepancy of Fig. 12 in the range of higher wave number between the eigenfunction expansion and our results can be attributed to the same number of boundary elements for all the cases of different wave numbers in our method. The case of higher wave number needs more number of elements in the BEM. However, the
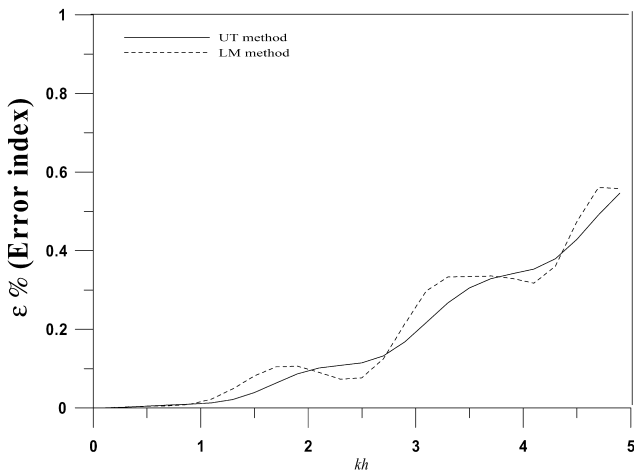
Fig. 14. The error index, $\epsilon\%$, versus *kh* for $\theta = 0°$ (example 2).
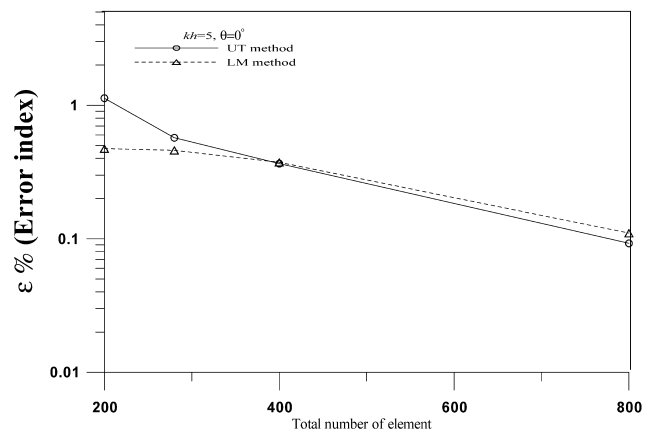
Fig. 15. The error index, $\epsilon\%$, versus the number of elements for the higher wave number ($kh = 5$) (example 2).

eigenfunction expansion method does not need boundary elements.

6. Conclusions

The dual integral formulation for the boundary value problem of the modified Helmholtz equation for solving the propagation of oblique incident wave passing a thin barrier (a degenerate boundary) has been derived in this paper. The properties of the potentials resulting from the four kernel functions in the dual integral equations have been examined, and their potential distributions have also been given. A DBEM program has been developed to solve for the water scattering problem passing a barrier. Two illustrative examples, a finite thickness and zero thickness barriers, have been successfully solved using the proposed DBEM, and the results were compared well with those obtained using analytical solutions and experiments.

References

[1] Abul-Azm AG. Diffraction through wide submerged breakwaters under oblique waves. Ocean Engng 1994;21(7):683–706.

[2] Buecker HF. Field singularities and related integral representations. In: Sih GC, editor. Mechanics of fracture, vol. 1. Noordhoff: Leyden; 1973.

[3] Chen JT, Chen KH, Chen CT. Adaptive boundary element method of time-harmonic exterior acoustics problems in two dimensions. Comput Meth Appl Mech Engng 2002;191:3331–45.

[4] Chen JT, Lin JH, Kuo SR, Chiu YP. Analytical study and numerical experiments for degenerate scale problems in boundary element method using degenerate kernels and circulants. Engng Anal Bound Elem 2001;25(9):819–28.

[5] Chen JT, Kuo SR, Lin GH. Analytical study and numerical experiments for degenerate scale problems in the boundary element method for two-dimensional elasticity. Int J Numer Meth Engng 2002;54:1669–81.

[6] Chen JT, Chen CT, Chen KH, Chen IL. On fictitious frequencies using dual BEM for non-uniform radiation problems of a cylinder. Mech Res Commun 2000;27(6):685–90.

[7] Chen JT, Hong H-K. Review of dual integral representations with emphasis on hypersingular integrals and divergent series. Appl Mech Rev 1999;52(1):17–33.

[8] Chen JT, Liang MT, Chen IL, Chyuan SW, Chen KH. Dual boundary element analysis of wave scattering from singularities. Wave Motion 1999;30:367–81.

[9] Chen JT, Kuo SR, Chen KH. A nonsingular formulation for the Helmholtz eigenproblems of a circular domain. J Chin Inst Eng 1999; 22(6):729–39.

[10] Chen JT, Huang CX, Chen KH. Determination of spurious eigenvalues and multiplicities of true eigenvalues using the real-part dual BEM. Comput Mech 1999;24:41–51.

[11] Chen JT, Wong FC. Dual formulation of multiple reciprocity method for the acoustic mode of a cavity with a thin partition. J Sound Vib 1998;217(1):75–95.

[12] Chen JT, Chen KH. Dual integral formulation for determining the acoustic modes of a two-dimensional cavity with a degenerate boundary. Engng Anal Bound Elem 1998;21:105–16.

[13] Chen JT, Chen KH, Yeih W, Shieh NC. Dual boundary element analysis for cracked bars under torsion. Engng Comput 1998;15(6): 732–49.

[14] Chen JT, Hong H-K. Dual boundary integral equations at a corner using contour approach around singularity. Adv Engng Software 1994;21(3):169–78.

[15] Chen JT, Hong H-K. On the dual integral representation of boundary value problem in Laplace equation. Bound Elem Abstr 1993;3:114–6.

[16] Chen JT, Hong H-K. Boundary element method, 2nd ed. Taipei: New World Press; 1992. in Chinese.

[17] Das P, Dolai DP, Mandal BN. Oblique wave diffraction by parallel thin vertical barriers with gaps. J Waterway Port Coast Ocean Engng (ASCE) 1997;123(4):163–71.

[18] Duhamel D, Sergent P. Sound propagation over noise barriers with absorbing ground. J Sound Vib 1998;218(5):799–823.

[19] Farina L, Martin PA. Scattering of water waves by a submerged disc using a hypersingular integral equation. Appl Ocean Res 1998;20: 121–34.

[20] Gray LJ. Boundary element method for regions with thin internal cavities. Engng Anal Bound Elem 1989;6(4):180–4.

[21] Günter NM. Potential theory and its applications to basic problems of mathematical physics. New York: Frederick Ungar Publishing Co; 1967.

[22] Hadamard J. Lectures on Cauchy's problem in linear partial differential equations. New York: Dover; 1952.

[23] Hong H-K, Chen JT. Derivations of integral equations of elasticity. J Engng Mech (ASCE) 1988;114(6):1028–44.

[24] Hsu HH, Wu YC. Scattering of water wave by a submerged horizontal plate and a submerged permeable breakwater. Ocean Engng 1999;26: 325–41.

[25] Ichiro HK. Open, partial reflection and incident-absorbing boundary conditions in wave analysis with a boundary integral method. Coast Engng 1997;30:281–98.

[26] Krishnasamy G, Rizzo FJ, Rudolphi TJ. Continuity requirements for density functions in the boundary element method for linear elasticity. Comput Mech 1992;9:267–84.

[27] Lafe OE, Montes JS, Cheng AHD, Liggett JA, Liu L-F. Singularities in Darcy flow through porous media. J Hydraul Div 1980;106: 977–96.

[28] Liang MT, Chen JT, Yang SS. Error estimation for boundary element method. Engng Anal Bound Elem 1999;23:257–65.

[29] Liu PLF, Wu J. Wave transmission through submerged apertures. J Waterway Port Coast Ocean Engng (ASCE) 1987;113(6):660–71.

[30] Liu PLF, Abbaspour M. An integral equation method for the diffraction of oblique wave by an infinite cylinder. Int J Numer Meth Engng 1982;18:1497–504.

[31] Liu PLF, Abbaspour M. Wave scattering by a rigid thin barrier. Proc Am Soc Civil Eng 1982;108:479–91.

[32] Losada IJ, Silva R, Losada MA. 3-D non-breaking regular wave interaction with submerged breakwaters. Coast Engng 1996;28: 229–48.

[33] Losada MA, Losada IJ, Roldan AJ. Propagation of oblique incident modulated waves past rigid, vertical thin barriers. Appl Ocean Res 1993;15:305–10.

[34] Losada IJ, Losada MA, Roldan AJ. Propagation of oblique incident waves past rigid vertical thin barriers. Appl Ocean Res 1992;14: 191–9.

[35] Mangler KW. Improper integrals in theoretical aerodynamics. RAE Rep 1951;2424.

[36] Martin PA, Rizzo FJ. Hypersingular integrals: how smooth must the density be? Int J Numer Meth Engng 1998;39(4):687–704.

[37] Martin PA, Rizzo FJ, Gonsalves IR. On hypersingular integral equations for certain problems in mechanics. Mech Res Commun 1989;16(2):65–71.

[38] Mciver P. Water-wave diffraction by thin porous breakwater. J Waterway Port Coast Ocean Engng (ASCE) 1999;125(2):66–70.

[39] Nakayama T. Boundary element analysis of nonlinear water wave problems. Int J Numer Meth Engng 1983;19:953–70.

[40] Ogilvie TF. Propagation of wave over an obstacle in water of finite depth. Berkley, CA: University of California/Institute of Engineering Research; 1960. p. 82.

[41] Ostry Diet I. Synthesis of a shaped-beam reflector antenna. In: Anderson RS, de Hoog FR, Lukas MA, editors. Application and numerical solution of integral equations. Alphena: Sijthoff & Noordhoff; 1980.

[42] Park JM, Eversman W. A boundary element method for propagation over absorbing boundaries. J Sound Vib 1994;175(2):197–218.

[43] Portela A. Dual boundary element analysis of crack. Comput Mech 1992;.

[44] Porter R, Evens DV. Complementary approximations to wave scattering by vertical barriers. J Fluid Mech 1995;294:155–80.

[45] Tanaka M, Sladek V, Sladek J. Regularization techniques applied to boundary element methods. Appl Mech Rev 1994;47(10):457–99.

[46] Terai T. On calculation of sound field around three dimensional objects by integral equation method. J Sound Vib 1980;69:71–100.

[47] Tuck EO. Application and solution of Cauchy singular integral equations. In: Anderson RS, de Hoog FR, Lukas MA, editors. Application and numerical solution of integral equations. Alphena: Sijthoff & Noordhoff; 1980.

[48] Wang CS, Chu S, Chen JT. Boundary element method for predicting storeairloads during its carriage and separation procedures. In: Grilli, Brebbia CA, Cheng AHD, editors. Computational engineering with boundary elements, fluid and potential problems. Computational Mechanics Publications; 1990.

[49] Wu TW, Wan GC. Numerical modelling of acoustic radiation and scattering from thin bodies using a Cauchy principal integral equation. J Acoust Soc Am 1992;92:2900–6.

[50] Yeih W, Chen JT, Chen KH, Wong FC. A study on the multiple reciprocity method and complex-valued formulation for the Helmholtz equation. Adv Engng Software 1998;29(1):7–12.

[51] Yueh CY, Tsaur DH. Wave scattering by submerged vertical plate-type breakwater using composite BEM. Coast Engng J 1999;41(1):65–83.